European Journal of Pharmaceutics and Biopharmaceutics 79 (2011) 635–645

Contents lists available at ScienceDirect

European Journal of Pharmaceutics and Biopharmaceutics

journal homepage: www.elsevier.com/locate/ejpb

Research paper

Development of sustained-release lipophilic calcium stearate pellets via hot melt extrusion

Eva Roblegg [a,b,*], Evelyn Jäger [b], Aden Hodzic [b], Gerold Koscher [b], Stefan Mohr [b], Andreas Zimmer [a], Johannes Khinast [b,c]

[a] Institute of Pharmaceutical Sciences, Department of Pharmaceutical Technology, Karl-Franzens University, Graz, Austria
[b] Research Center Pharmaceutical Engineering, Graz, Austria
[c] Institute for Process and Particle Engineering, Graz, University of Technology, Austria

ARTICLE INFO

Article history:
Received 27 May 2011
Accepted in revised form 11 July 2011
Available online 21 July 2011

Keywords:
Calcium stearate
Retarded drug release
Paracetamol
Glyceryl monostearate
Tributyl citrate

ABSTRACT

The objective of this study was the development of retarded release pellets using vegetable calcium stearate (CaSt) as a thermoplastic excipient. The matrix carrier was hot melt extruded and pelletized with a hot-strand cutter in a one step continuous process. Vegetable CaSt was extruded at temperatures between 100 and 130 °C, since at these temperatures cutable extrudates with a suitable melt viscosity may be obtained. Pellets with a drug loading of 20% paracetamol released 11.54% of the drug after 8 h due to the great densification of the pellets. As expected, the drug release was influenced by the pellet size and the drug loading. To increase the release rate, functional additives were necessary. Therefore, two plasticizers including glyceryl monostearate (GMS) and tributyl citrate (TBC) were investigated for plasticization efficiency and impact on the in vitro drug release. GMS increased the release rate due to the formation of pores at the surface (after dissolution) and showed no influence on the process parameters. The addition of TBC increased the drug release to a higher extent. After dissolving, the pellets exhibited pores at the surface and in the inner layer. Small- and Wide-Angle X-ray Scattering (SWAXS) revealed no major change in crystalline peaks. The results demonstrated that (nearly) spherical CaSt pellets could be successfully prepared by hot melt extrusion using a hot-strand cutter as downstreaming system. Paracetamol did not melt during the process indicating a solid suspension. Due to the addition of plasticizers, the in vitro release rate could be tailored as desired.

1. Introduction

Pellets are defined as small, free-flowing, spherical, or semi-spherical units made of fine powders or granules of a diameter between 0.5 and 1.5 mm [1] that must have a desired set of properties. They facilitate administration, individual dosing, controlled release, and taste masking and thus, improve patient compliance. Pellets can be produced via the extrusion/spheronization technique. Wet extrusion typically involves the use of granulation liquids, which often requires specialized equipment due to flammability and residue of organic solvents. Furthermore, the processing times are long because of the wetting and drying stages [2] involved. Such disadvantages can be overcome by hot melt extrusion (HME), an innovative technology for the production of a variety of dosage forms, including implants [3], tablets [4], pellets [5], and films [6]. Despite its name, melts are often not hot, and sometimes the carrier systems are not even melted, e.g., in the extrusion of lipids. Melt extrusion processes have been used in the industry for many years, the production of thin films in the plastics industry being only one of the most prominent examples. HME has also found numerous applications in pharmaceutical manufacturing practice [4,7–9]. Compared to other pharmaceutical production processes, HME has the benefit of being a solvent-free, environmental friendly, and cost-efficient technology. Furthermore, HME improves bioavailability by forming solid dispersions and solid solutions. This is relevant for poorly soluble pharmaceutically compounds, frequently encountered among new active ingredients [10–12].

A formulation for hot melt extruded pellets typically comprises a matrix and an active pharmaceutical ingredient (API), as well as other components, such as plasticizers, anti-tacking agents, pore formers, colorants, stabilizers and others. A typical HME process consists of a feeding system, an extruder with a conveying, mixing, and melting sections, a die section, and further downstream processing units, such as hot-strand cutters or calendaring. Thus, a pharmaceutical carrier system processed by HME must deform inside the extruder and solidify at the outlet. The die at the end

* Corresponding author. Karl-Franzens University, Institute of Pharmaceutical Sciences, Department of Pharmaceutical Technology, Universitätsplatz 1, 8010 Graz, Austria. Tel.: +43 316 380 8888; fax: +43 316 380 9100.
E-mail address: eva.roblegg@uni-graz.at (E. Roblegg).

0939-6411/$ - see front matter © 2011 Elsevier B.V. All rights reserved.
doi:10.1016/j.ejpb.2011.07.004

of the extruder determines the form of the extrudate. Depending on the viscoelastic properties of the used material, die swelling (i.e., increasing in the radius) can occur [7]. Carriers that are generally used are (thermoplastic) polymers (water-soluble and water-insoluble) and waxes or wax-based materials, which control the process and the release (mechanism) of the drug from the final dosage form [7].

Among these carriers, lipids are promising excipients for the preparation of controlled-release systems. They are biodegradable and can mask the bitter taste of drugs [13]. Additionally, they may improve drug absorption in the gastrointestinal tract, which is beneficial for low therapeutic index drugs [14]. Furthermore, the lipophilic carrier may protect water-sensitive drugs from hydrolysis [15]. For example, Schroeder et al. [16] evaluated the melting characteristics of several drugs mixed with carnauba and castor wax to assess possible eutectic formations. The results demonstrated that the interactions were strictly physical and that the physical characteristics influenced the release of the drug from the waxy matrix. Sato et al. [17] and Miyagawaa et al. [18] prepared granules of carnauba wax (with diclofenac sodium) in a twin-screw compounding extruder at temperatures below the melting point (T_m 85 °C). To increase the drug release from the granules, rate-controlling agents (i.e., hydroxypropylcellulose, Eudragit, sodium chloride) were added to evaluate the influence of swelling and solubility effects on dissolution profiles. The results showed that the selection of a functional additive (based on its physicochemical properties) is essential for the preparation of dosage forms with desired dissolution profiles. The usage of glyceryl monostearate (GMS) as a lipid carrier system has also been reported in the literature [19]. GMS has a melting point between 55 and 60 °C and shows emulsifying and plasticizing effects. Thomsen et al. [15] reported pellets containing various hydrophobic meltable substances and paracetamol produced with a high-shear mixer. These pellets were expected to reveal a prolonged release profile since GMS is insoluble in water. The results demonstrated that GMS displayed favorable plasticizing characteristics for the process. However, the sustained-release profile of the water-soluble model drug paracetamol could only be achieved by including microcrystalline wax.

In this work, calcium stearate (CaSt) was chosen as a matrix that is generally used as a lubricant in tablets and capsules. CaSt is a mixture of insoluble calcium salts of various fatty acids, mainly consisting of stearic and palmitic acids and minor proportions of other fatty acids [19]. Previous work has shown that CaSt can be used as pelletization aid for retarded release formulations prepared via wet extrusion/spheronization [20]. Due to the high plasticity of this material, spherical pellets with a narrow size distribution were obtained. Since CaSt softens between 120 and 130 °C and exhibits a viscous consistency at higher temperature [19], this material may be a new candidate for HME. Thus, the objective of the current study was to develop retarded release pellets using vegetable CaSt as a novel hot melt extrusion excipient. The goal was to obtain a solid suspension (i.e., the API does not melt, and API crystals remain intact and are embedded in the matrix). Additionally, two plasticizers, i.e., GMS and tributyl citrate (TBC) were incorporated into the matrix carrier to evaluate the efficiency of plasticization and its influence on the release properties. Thermal properties, crystallinity, compatibility, and processability (effect of drug content and plasticizers on the hot melt extrusion process) were studied. The pellets were characterized using sieve and image analyses, Small- and Wide-Angle X-ray Scattering (SWAXS), and Scanning Electron Microscopy (SEM). The dissolution profile of a water-soluble model drug was determined, and the effect of plasticizers and drug loading on the in vitro release was evaluated.

2. Materials and methods

2.1. Materials

Paracetamol of European Pharmacopeia grade (EP) was donated by G.L. Pharma GmbH, Lannach, Austria (volume mean particle size 139.2 μm). CaSt (stearic acid 44% and palmitic acid 54%, EP, Werba-Chem GmbH, Vienna, Austria; mean particle size 16.62 μm) was used as a matrix carrier system. The plasticizers for this study were GMS (solid state, Apoka, Vienna, Austria, mean particle size 18.23 μm) and TBC (liquid state, Merck, Darmstadt, Germany, density). In vitro release studies were carried out with 0.1 N hydrochloric acid (Merck, Darmstadt, Germany) and trisodiumphosphate-dodecahydrate buffer (Merck, Darmstadt, Germany) to simulate gastric and intestinal conditions. For the solvent evaporation method, acetone was purchased from Carl Roth GmbH, Karlsruhe, Germany. For the reversed phase high-performance liquid chromatography, ammonium dihydrogenphosphate and ammonium hydrogenphosphate (Fluka, Sigma Aldrich Chemicals, St. Louis, MO, USA), phosphoric acid (85%, VWR international, Darmstadt, Germany), and methanol (LiChrosolv®Reag., EP, VWR international, Darmstadt, Germany) were used as the mobile phase.

2.2. Powder characterization

Pure substances (i.e., paracetamol, CaSt, TBC, GMS, and physical mixtures) were investigated via differential scanning calorimetry (DSC) and SWAXS to determine melting temperatures (T_m), degradation temperatures (T_{deg}), incompatibilities, and crystallinity.

2.2.1. T_m, T_{deg} and incompatibility studies using DSC/HPLC

Powder samples of the pure starting materials (5–8 mg, $n = 3$) were placed into aluminium crucibles, which were closed, pierced, and purged with pure nitrogen. Physical mixtures were obtained by pre-mixing at room temperature for 20 min at 60 Hz using a turbula mixer (Turbula® TypT2F, Turbula System Schatz, Willy Bachofen AG, Muttenz, Switzerland). For the sample preparation of the liquid plasticizing agent TBC, a solvent evaporation method was used [21]. For this, 0.25–0.5 g TBC was mixed with 20 ml acetone. Subsequently, the matrix carrier system CaSt (2.5–4.5 g) and paracetamol (1–2 g), which were dissolved in TBC/acetone in Petri dishes and transferred into an exsiccator, were added. For 1 h, the exsiccator was flushed with nitrogen, followed by evacuation for 12 h at 35 mbar. Samples of the prepared mixtures (5–8 mg, $n = 2$) were extracted from the Petri dishes and used for the DSC measurements (204F1 Phoenix®, Netzsch GmbH, Selb, Germany). The scanning rate for all samples was 5 K/min from 25 to 200 °C. After cooling (5 K/min) to 25 °C, a second run was performed. An empty aluminum crucible was used as a reference. The DSC data were analyzed with Proteus Thermal Analysis software (Netzsch GmbH, Selb, Germany). For the incompatibility studies, after the first cycle, DSC crucibles of the physical mixtures were opened with a scalpel blade, scraped off the pans, and transferred into a 1.5 ml glass vial containing 700 μl mobile phase (see HPLC analysis). The samples were extracted for 10 min from the ultrasonic bath, subsequently filtered through a 0.45 Mm regenerated cellulose syringe filter (Carl Roth GmbH, Karlsruhe, Germany), and injected into the HPLC system.

2.3. Hot melt extrusion process

Hot melt extrusion was performed using a co-rotating twin-screw extruder (Coperion, Stuttgart, Germany). The extruder

consisted of two rotating, intermeshing 18 mm screws (D_o/D_i = 1.55) inside of a cylindrical barrel. This barrel was composed of 10 sections (barrel zones), which were bolted together and heated individually with electric heaters. The set temperatures of the individual barrels (70–130 °C, depending on the formulation) are listed in Table 2. The screw was designed to fulfill the following basic functions: (i) to move the material along the screw (conveying element), (ii) to soften (and partially melt) the material (right-handed kneading element), (iii) to mix the soft material melt (conveying, right- and left-handed kneading elements), (iv) to meter the melt to the die area (conveying element), and (v) to apply a constant pressure to force the material through the die. Two die plates (with each having two identical holes) with different hole diameters, i.e., 1.0 and 1.5 mm were employed for the experiments. Degassing of the mass was conducted for all experiments in the barrel-zone 9. The throughput was 0.5 kg/h, and all extrusions were carried out at the screw speed of 200 rpm. Subsequently, the extrudates were cut into small cylinders using a hot-strand cutter with two rotating knives (ZGF30, Coperion, Stuttgart, Germany) and cooled with an external cooling system (oil-free compressed air). To obtain pellets in the desired size of 1.0 and 1.5 mm, the rotational speed of the knives was set manually (dependent on the formulation). The extruder and the configuration of the co-rotating screw are illustrated in Fig. 1.

2.3.1. Preparation of unloaded melt extruded pellets

To evaluate the suitability of CaSt as a lipophilic pelletization aid for hot melt extrusion, during the first set of experiments, unloaded formulations (500 g) containing CaSt and CaSt/GMS (5%) were blended in a turbula mixer at 60 Hz for 20 min. The powder or the powder mixture (500 g) was filled into a dosing device (K-Tron, K-PH-CL-24-KT-20, K-Tron, Niederlenz, Switzerland) and gravimetrically fed into the barrel-zone 1 of the co-rotating twin-screw extruder. A liquid plasticizer TBC (5% and 10%) was added to the matrix carrier CaSt during the extrusion process with a HPLC pump (Jasco PU-980, Groß-Umstadt, Germany) at barrel-zone 3 (side-feeder). The extrusion process was conducted as described above. All unloaded formulations and processing parameters are listed in Tables 1 and 2.

2.3.2. Preparation of drug-loaded melt extruded pellets

Powder blends for extrusion were prepared by pre-mixing the matrix carrier CaSt with each of the plasticizers (addition of TBC during the extrusion process at barrel-zone 3) and the model drug paracetamol (20% and 40% drug loading) in a turbula mixer at 60 Hz for 20 min. The extrusion process was carried out in the same device as for the unloaded formulations. At the end of the die, the extrudates were hot face cut into small pellets and externally cooled. All formulations and process parameters are listed in Tables 1 and 2.

2.4. Pellet characterization

2.4.1. Sieving and image analysis

Each formulation was sieved according to the European Pharmacopeia 6.0 (2.9.3.) to define the yield fractions (i.e., 1.0–1.25 mm and 1.4–1.6 mm). In brief, the samples were sieved with seven analytical DIN sieves of 630–1800 μm aperture (Type RV,

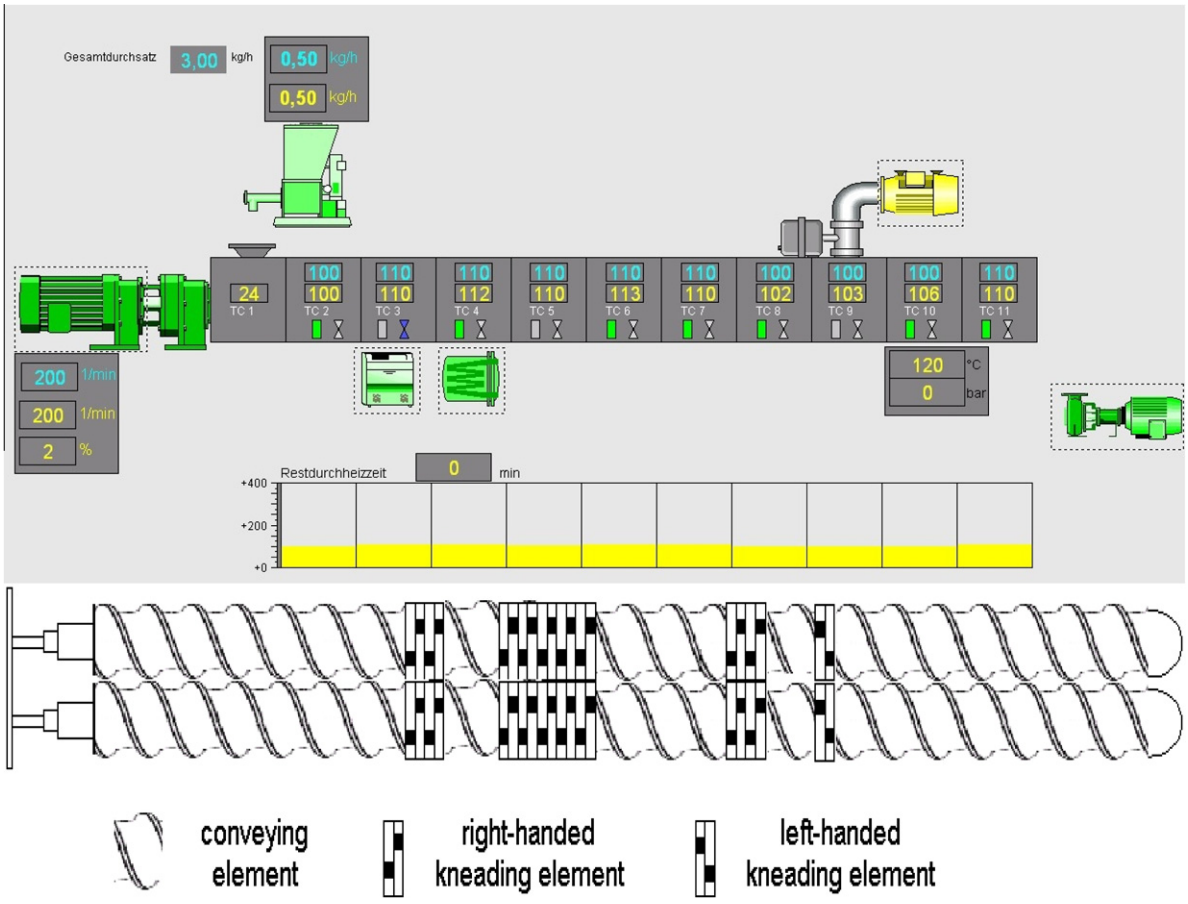

Fig. 1. Schematic illustration of the extruder (including feed rates and set temperatures) and configuration of the co-rotating screw. (For interpretation of the references to color in this figure legend, the reader is referred to the web version of this article.)

Table 1
Composition of blends processed by HME using two different die plates (i.e., 1.0 mm and 1.5 mm).

Abbreviation	CaSt (% (w/w))	Paracetamol (% (w/w))	GMS (% (w/w))	TBC (% (w/w))	Die diameter (mm)
CaSt_1	100				1.0
CaSt_1.5	100				1.5
CaSt/G5%_1	95		5		1.0
CaSt/G5%_1.5	95		5		1.5
CaSt/T5%_1	95			5	1.0
CaSt/T5%_1.5	95			5	1.5
CaSt/T10%_1	90			10	1.0
CaSt/T10%_1.5	90			10	1.5
CaSt/P20%_1	80	20			1.0
CaSt/P20%_1.5	80	20			1.5
CaSt/P40%_1	60	40			1.0
CaSt/P40%_1.5	60	40			1.5
CaSt/P20%/G5%_1	75	20	5		1.0
CaSt/P20%/G5%_1.5	75	20	5		1.5
CaSt/P40%/G5%_1	55	40	5		1.0
CaSt/P40%/G5%_1.5	55	40	5		1.5
CaSt/P20%/T5%_1	75	20		5	1.0
CaSt/P20%/T5%_1.5	75	20		5	1.5
CaSt/P40%/T5%_1	55	40		5	1.0
CaSt/P40%/T5%_1.5	55	40		5	1.5
CaSt/P20%/T10%_1	70	20		10	1.0
CaSt/P20%/T10%_1.5	70	20		10	1.5
CaSt/P40%/T10%_1	50	40		10	1.0
CaSt/P40%/T10%_1.5	50	40		10	1.5

Table 2
Process parameters applied in the formulation design. The rotational speed was set at 200 rpm.

Abbreviation	Process parameter												Sieving and image analysis		
	Amount (kg/h)	Torque (%)	Barrel-zone temperatures (°C)										Rotational speed of the knives (rpm)	Pellet yield (%)	d_{Fer} (mm)	AR (–)
			1	2	3	4	5	6	7	8	9	10				
CaSt_1	0.5	12	100	110	100	110	110	110	100	100	100	110	1540	66.17	1.210	1.17
CaSt_1.5	0.5	12	100	110	100	110	110	110	100	100	100	110	850	62.30	1.832	1.25
CaSt/G5%_1	0.5	13	90	100	110	110	110	110	100	90	90	100	1950	70.13	1.253	1.18
CaSt/G5%_1.5	0.5	13	90	100	110	110	110	110	100	90	90	100	1120	67.93	1.867	1.21
CaSt/T5%_1	0.5	14	80	90	90	90	90	90	80	80	80	100	1930	71.87	1.233	1.26
CaSt/T5%_1.5	0.5	14	80	90	90	90	90	90	80	80	80	100	1120	66.47	1.942	1.27
CaSt/T10%_1	0.5	10	70	70	70	70	70	70	60	60	60	90	2360	64.10	1.367	1.21
CaSt/T10%_1.5	0.5	10	70	70	70	70	70	70	60	60	60	90	1690	64.97	n.m.	n.m.
CaSt/P20%_1	0.5	16	100	110	130	130	130	130	120	110	100	110	1300	74.78	1.460	1.20
CaSt/P20%_1.5	0.5	16	100	110	130	130	130	130	120	110	100	110	610	79.70	1.878	1.26
CaSt/P40%_1	0.5	24	100	110	130	130	130	130	120	110	100	110	1700	65.67	1.385	1.26
CaSt/P40%_1.5	0.5	24	100	110	130	130	130	130	120	110	100	110	1150	63.00	1.849	1.20
CaSt/P20%/G5%_1	0.5	14	90	100	110	110	110	110	100	90	90	90	2560	69.78	1.329	1.24
CaSt/P20%/G5%_1.5	0.5	14	90	100	110	110	110	110	100	90	90	90	1980	64.85	1.656	1.20
CaSt/P40%/G5%_1	0.5	10	90	100	110	110	110	110	100	90	90	90	1950	60.48	1.231	1.22
CaSt/P40%/G5%_1.5	0.5	10	90	100	110	110	110	110	100	90	90	90	1120	63.55	1.798	1.18
CaSt/P20%/T5%_1	0.5	13	110	130	130	120	120	120	120	120	120	120	1850	74.08	1.276	1.18
CaSt/P20%/T5%_1.5	0.5	13	110	130	130	120	120	120	120	120	120	120	600	63.75	1.801	1.10
CaSt/P40%/T5%_1	0.5	13	110	130	130	120	120	120	120	120	120	120	1950	72.07	1.165	1.22
CaSt/P40%/T5%_1.5	0.5	13	110	130	130	120	120	120	120	120	120	120	590	63.11	1.887	1.18
CaSt/P20%/T10%_1	0.5	8	110	120	140	140	140	140	130	100	80	100	2930	63.21	1.484	1.22
CaSt/P20%/T10%_1.5	0.5	8	110	120	140	140	140	140	130	100	80	100	1390	62.60	1.810	1.25
CaSt/P40%/T10%_1	0.5	6	110	120	140	140	140	140	130	100	80	100	970	57.63	1.089	1.28
CaSt/P40%/T10%_1.5	0.5	6	110	120	140	140	140	140	130	100	80	100	580	62.12	1.814	1.23

Retsch KG, Haan, Germany) at an agitation of 50 vibrations per minute until the endpoint was reached. Subsequently, a representative sample of each fraction (15 g) was obtained. For the performance of the image analysis, the high-speed image analysis system QICPIC with a RODOS dry disperser and a VIBRI dry feeder was used (QICPIC, Sympatec GmbH, Clausthal-Zellerfeld, Germany). Pellet size and shape were determined in terms of mean Feret's diameter and the aspect ratio (AR).

2.4.2. Pellet structure

The extruded pellets were characterized via SWAXS. A Hecus SWAXS system (HECUS S3-MICRO) was used for investigating the structure of the materials. The SWAXS (SAXS and WAXS) system consists of a high-flux laboratory SWAXS camera S3-Micro (Hecus X-ray Systems, Graz Austria). This system is equipped with a high-brilliance microbeam delivery system, operating at a low power of 50 W (50 kV and 1 mA) with point-focus optics (FOX3D, Xenocs, Grenoble, France) and with a 1D- or 2D-detection system. The apparatus is combined with automated data evaluation software. The X-ray wavelength λ used in this study was 1.54 Å, and the SAXS and WAXS curves (scattering intensities as a function of the scattering angle 2θ) were recorded with two independent 1D detectors (PSD-50, Hecus X-ray Systems, Graz, Austria) in the angular range of $0.06° < 2\theta < 8°$ and $17° < 2\theta < 27°$. The q-scale was related to the scattering angle 2θ by $q = 4\pi * \sin\theta/\lambda$ [22] and represented the magnitude of the reciprocal scattering vector.

The calibration of the *q*-scale, i.e., the calibration of the detector pixels to the respective scattering angle, was performed by measuring silver behenate with a defined lamellar spacing of 58.38 Å in the SAXS range and p-bromo-benzoic-acid in the WAXS range. For the measurements, the samples were filled into glass capillaries with an inner diameter of 2 mm, sealed with wax, and placed into the SpinCap.

2.4.3. In vitro drug release studies

All dissolution experiments were examined in vitro by the USP 28 rotating basket method ⟨711⟩ (Pharma Test PTWS III C, Pharma Test AG, Hainburg, Germany). The apparatus was used at a release temperature of 37 ± 0.5 °C and a rotational speed of 100 rpm. The dissolution medium consisted of 750 ml 0.1 N hydrochloric acid. After 2 h, 250 ml trisodiumphosphate-dodecahydrate buffer was added to switch the pH from 1.2 to 6.8. For each drug-loaded formulation, 1 g of pellets was transferred into the basket. The dissolution characteristics of each formulation were determined sixfold. Samples of 1 ml were withdrawn from the dissolution medium after 10 min (initial dose), followed by sampling at 0.5, 1, 2, 3, 4, 5, 6, 7, 8, and 24 h. All samples were analyzed via reversed phase high-performance liquid chromatography (RP-HPLC).

2.4.4. RP-HPLC analysis

The HPLC analysis was carried out with a HP1090 liquid chromatography (Hewlett Packard, Palo Alto, CA, USA) equipped with a diode array detector (detection at 272 nm). A reversed phase ODS silica column (125 × 4 mm, LiChrospher®, 5 μm RP-18, 100 Å pore size, VWR international, Darmstadt, Germany) was used as the stationary phase. The mobile phase consisted of an aqueous solution containing 7.6 mM ammonium hydrogenphosphate and 5.4 mM ammonium dihydrogenphosphate. The mixture was adjusted with phosphoric acid to pH 2.6 and was diluted with methanol at the ratio of 60:40 (w/w). Prior to use, the mobile phase was filtered through a cellulose nitrate filter (Sartorius, Göttingen, Germany) with a pore size of 0.2 μm and degassed with helium (purity: 5.0) for 10 min. Samples (5–10 μl) were injected automatically with an autosampler, and the flow rate was set to 0.8 ml/min. The quantification of the dissolution samples was performed by a single-point calibration with a 100% standard solution of the used API paracetamol.

2.4.5. Mechanism of drug release

In order to evaluate the kinetics of drug release from the melt extruded pellets, various models were tested. The obtained dissolution profiles (selected sections) were fitted according to (i) zero-order kinetics, (ii) first-order kinetics, (iii) Higuchi model, and (iv) the Korsmeyer–Peppas model. These models are described elsewhere, e.g., [23]. SigmaPlot Version 11 (SysStat) was used for data fitting.

2.4.6. Pellet structure

The surface and internal structure of the produced pellets (with and without paracetamol) were investigated via SEM. The pellets were analyzed after the extrusion process and after the performed in vitro release studies (24 h). For this analysis, the pellets were cut mechanically with a scalpel. The intact and cut pellets were mounted on stubs using a double-sided sticky band, followed by sputter coating with chromium and an examination in a scanning electron microscope (Zeiss Ultra 55, Carl Zeiss NTS GmbH, Oberkochen, Germany).

3. Results and discussion

The preparation of hot melt extruded pellets requires the use of a thermoplastic matrix system. Thus, the material must be able to deform in the extruder and solidify at the end of the process [7]. In this study, the suitability of CaSt as a hot melt extrusion excipient was evaluated. CaSt is a mixture of insoluble calcium salts of different fatty acids, mainly consisting of stearic and palmitic acids and minor proportions of other fatty acids [19].

3.1. Thermal behavior of the CaSt powder

CaSt exhibits several thermotropic crystalline and mesomorphic phase transitions [24] and decomposes at 350 °C [25]. Vold et al. [25] reported microscopic visual observations during heating and cooling of CaSt. No visual changes were detected below 123 °C. At this temperature, particles started to coalesce and CaSt became translucent. At 150 °C, the matrix carrier became almost transparent with a pebbly (stony) structure. Increasing the temperature to 195 °C, thread-like spots appeared and the sample became brighter at the same time. The same characteristics were observed on cooling. In this study, the thermal behavior of CaSt was investigated by DSC measurements (see Fig. 2). The thermogram of the first heating cycle demonstrated the following four peaks: at 20.3 °C, at 120 °C, at 163.9 °C, and at 196 °C. The exothermic peak at 20.3 °C derived from $\alpha 1 \rightarrow \alpha 0$ phase transition [26]. The latter one is the stable form at room temperature. The endothermic peak appearing at 120.7 °C was associated with a structural rearrangement reaching a mesomorphic state, i.e., the transition of the solid crystalline state in the liquid crystalline one. This effect is also confirmed by other studies [27]. The mesomorphic state is divided into two classes: the smectic (soap-like) and the nematic (thread-like) states. The transition of the smectic mesophase into the nematic is indicated by the endothermic peak at 163.9 °C. The signal at 196.3 °C was due to the transition of the nematic state into the liquid state. These findings are in accordance with the literature [27]. The cooling rate was 5 K/min from above 200 °C to 0 °C. The first transformation was detected at 173.4 °C. This transformation was reversible on cooling and reproducible at repeated heating (196.3 °C). No transformations at 163.9 °C and 123 °C were observed during cooling, which might be due to the low heats of transformations and/or second-order transitions [25]. In the second heating cycle, however, both endothermic peaks were reproducible. The second exothermic peak appearing at 37.0 °C on cooling was observed as a result of the thermal treatment of the

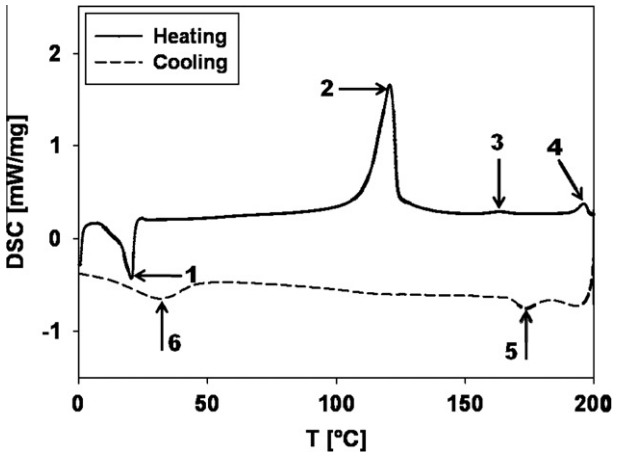

Fig. 2. DSC thermogram of the first heating cycle and the cooling cycle of CaSt, (1) exothermic peak at 20.3 °C ($\alpha 1 \rightarrow \alpha 0$ phase transition), (2) endothermic peak at 120.7 °C (structural rearrangement, i.e., the transition of the crystalline state into the liquid crystalline state, (3) endothermic peak at 163.9 °C (smectic mesophase becomes nematic), (4) endothermic peak at 196.3 °C (transition of the nematic state into the liquid state), the cooling curve displayed two exothermic peaks, (5) at 173.4 °C and 6: at 37 °C.

α phase. The hydrated α0 phase was transformed into a mixture of β and γ [26]. The results of the compatibility tests showed that CaSt demonstrated no incompatibilities. The degradation temperatures were well above 200 °C for CaSt, paracetamol, and the functional additives.

3.2. Influence of drug content and plasticizers on the hot melt extrusion process

In order to determine the temperature to obtain extrudates with the right viscosity for the formation of a strand suitable for hot-face cutting, pure CaSt was extruded at a temperature between 100 and 110 °C (viscosity: 504.167 Pa s). Thus, the barrel temperature (which can be set in the extruder process controller) was chosen to result in a material that can be extruded and cut at the die. The rotational speed was set to 200 rpm (for all formulations), and the evaluated torque values were 12%. All process parameters are listed in Table 2. Adding GMS to the matrix carrier reduced the necessary set process temperature slightly (90–110 °C) but had no effect on the torque. TBC, the liquid plasticizer, was added to the matrix carrier CaSt during the extrusion process with a HPLC pump in two concentrations (i.e., 5% and 10%). With increasing amount of TBC, the required process temperature decreased from 80–90 °C to 60–70 °C due to a decrease in the viscosity of the matrix carrier. This temperature decrease was due to the high plasticizing effect of TBC (in dependence of the concentration), resulting in the right melt viscosity of the matrix carrier. Furthermore, higher TBC concentrations decreased the torque to 10%.

Next, paracetamol was incorporated into CaSt. The required process temperature was 100–130 °C regardless of the drug concentration. With exception of the torque, all parameters remained constant. With increasing concentration of paracetamol, the torque increased to 16% and 24%. It is reported in the literature that paracetamol shows plasticizing effects, resulting in lower required process temperatures and lower torque values. In their study, Qi et al. [28] described plasticizing properties of paracetamol in case of hot melt extruded Eudragit® E. The glass transition of the dispersion was considerably lower than the polymer alone, indicating dispersion of the drug in the polymer on a molecular basis. Similar effects have been described for ibuprofen [29]. Our results demonstrate that due to the process temperature of 100–130 °C, paracetamol did not melt during the process; thus, the drug was dispersed in CaSt and did not affect (i.e., by plasticizing) the matrix carrier. Instead, the presence of solid particles increased the effective viscosity of the system, leading to higher torques.

The formulations with GMS and TBC in combination with the model drug were extruded at the same temperatures. With an increasing amount of TBC, the torque was reduced to 6%. No swelling effects occurred in all formulations, indicating a high viscous and low elastic contribution of the CaSt formulation during extrusion [30].

In order to obtain pellets, a downstreaming system (to shape the thermoplastic strands) must be used. A variety of downstreaming systems, including dry strand pelletization, underwater pelletization, milling, and spheronization, are available. The latter requires special mechanical properties of the extrudates, i.e., brittleness to break into rods, and plasticity, to be rounded [31]. In this study, a hot-strand cutter with two rotating knives was used to obtain (nearly spherical) pellets with a narrow size distribution. The rotational speed of the knives was set between 580 and 2930 rpm, depending on the throughput and the desired pellet size. With the increasing size of the die, the rotational speed decreased. Subsequently, a sieve analysis of the cool pellets was performed. The obtained pellet size distributions demonstrated that all of the investigated formulations produced with the 1 mm die had a yield between 57.63% and 74.78% in the desired size fraction of 1.0–1.25 mm. The pellets prepared with the 1.5 mm die had a yield between 62.12% and 79.7% in the size fraction of 1.4–1.6 mm. For each formulation, the median Feret's diameter and the median aspect ratio (AR) were determined (Table 2). All Ferret's diameters of pellets produced with the 1 mm die were above 1.25 mm, with the exception of CaSt_1, CaSt/G5%_1, CaSt/T5%_1, CaSt/P40%/G5%_1, CaSt/P40%/T5%_1, and CaSt/P40%/T10%_1. Aspect ratio is defined as the ratio of the length of a pellet divided by the width, with pellets being considered spherical if the aspect ratio is between 1 and 1.2 [32]. ARs were suitable (i.e., $\leqslant$1.2) for pure CaSt pellets, CaSt and GMS pellets, CaSt pellets loaded with 20% paracetamol, and pellets composed of CaSt, 20% drug, and small amounts of TBC. No formulations (prepared with the 1 mm die) showed AR values above 1.28, indicating that the pellets were (nearly) spherical. All pellet formulations produced with the 1.5 mm die showed Feret's diameter above 1.6 mm. The ARs were satisfactory (i.e., $\leqslant$1.27) with the exception of CaSt/T10%_1.5 (formation of aggregates in the injector). For the unloaded pellets, it was assessed that GMS showed no influence on the AR compared to the pure CaSt pellets. Adding TBC increased the ARs. This effect was more pronounced with increasing TBC concentration. In general, TBC showed a higher plasticizing effect, indicating that the pellets slightly deform during the cutting process. The incorporation of paracetamol into the CaSt–TBC formulations decreased the ARs due to a decreased formability behavior of the pellets since the drug did not melt in the matrix carrier. The produced unloaded and loaded pellets (with 20% drug) are depicted in Fig. 4.

3.3. Structure characterization of the pellet formulations

The structure of the materials in the extruded pellets was examined via SWAXS (Fig. 3). Pure CaSt pellets displayed a visible Bragg peak in the angular WAXS region at 4.2 Å. Comparing the Bragg peak of the pure powder with the CaSt pellet showed the same peak position but a higher degree of the structural order (crystallinity) of the pellets due to mechanical treatment of CaSt during extrusion (Fig. 3A). This stronger crystal lattice is expected to yield a higher stability of CaSt pellets. Furthermore, the SAXS pattern of CaSt pellets showed 4 lamellar peaks at 47.1, 23.8, 15.9, and 12.0 Å (Fig. 3B). Compared with the CaSt powder, no peak shifts occurred, demonstrating that CaSt did not reach the mesomorphic state, i.e., the transition of the solid crystalline state in the liquid crystalline state during the extrusion process at 110 °C (barrel temperature). As a consequence, due to the lubricating effect of CaSt, which is intimately related to its rheology, the shear forces between the rotating screws and the wall of the barrel seemed to be small.

Pure paracetamol exhibits crystallinity peaks in the WAXS spectrum at 4.9, 4.4, 3.8, 3.7, 3.4, and 3.3 Å. After thermal processing, the paracetamol peaks remained in the same positions (Fig. 3C and D). Thus, it can be assumed that paracetamol did not melt during the extrusion process and was embedded in CaSt in its crystalline form. The addition of GMS did not influence the API since all crystalline peaks in the WAXS spectrum showed the same values (Fig. 3E). The SAXS pattern exhibited 4 lamellar peaks for CaSt, which were in the same angular positions as the corresponding powder sample (Fig. 3F). The lamellarity of GMS in the SAXS angular region showed a shift compared with the untreated GMS, which can be attributed to the dominance of the CaSt lattice. TBC, an amorphous liquid, showed no influence on the crystallinity of CaSt and paracetamol (Fig. 3G and H). No peak shift could be detected. In conclusion, paracetamol was embedded in CaSt in its crystalline form. The incorporation of GMS and TBC showed no impact on the crystallinity for both CaSt and the drug.

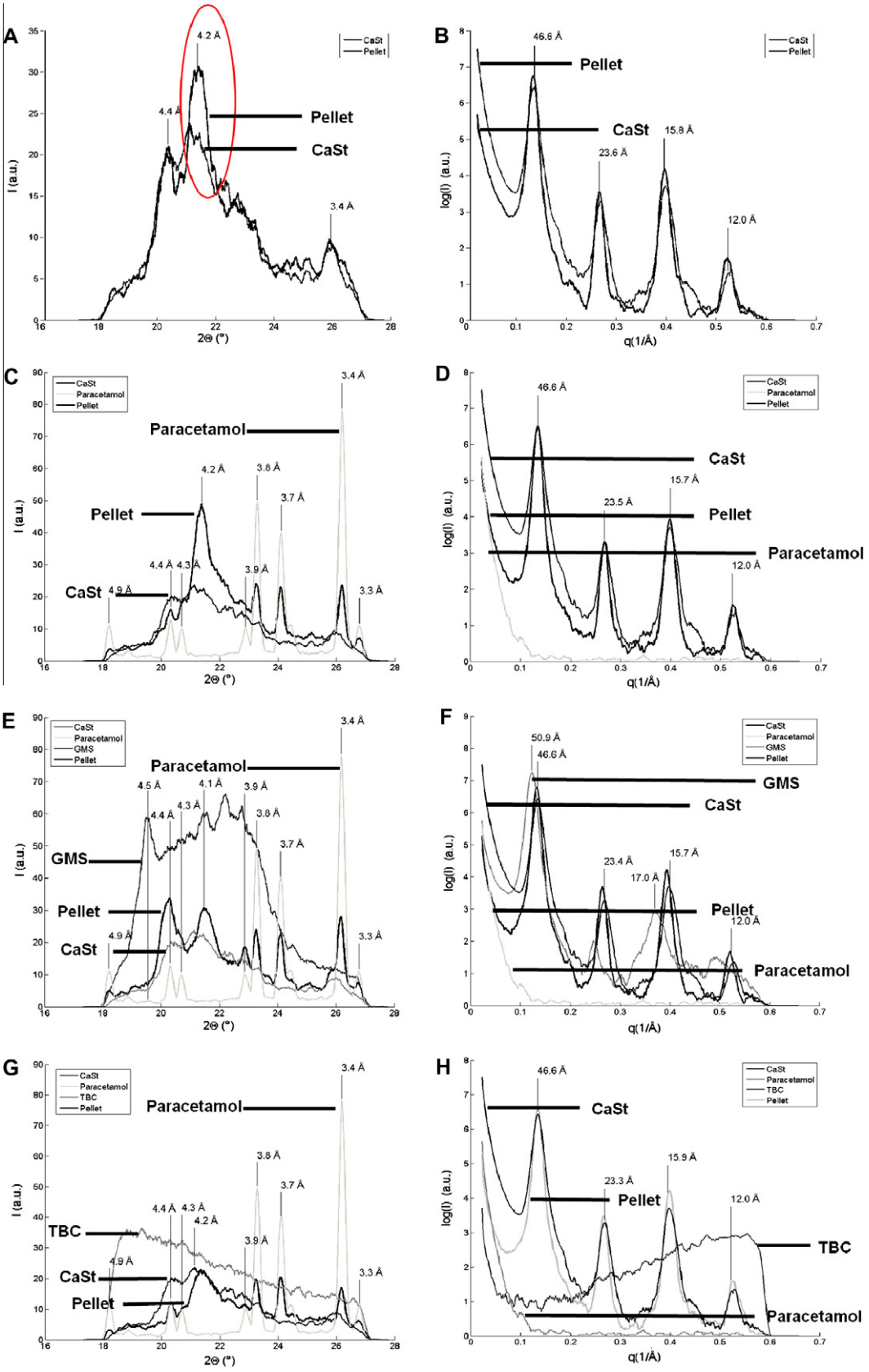

Fig. 3. SWAXS spectra of pure substances and pellets (A) CaSt powder and CaSt pellets WAXS spectrum: The circle indicates the higher degree of the structural order for pellets at 4.2 Å and (B) SAXS spectrum, (C) CaSt powder, paracetamol (P) powder, and CaSt–paracetamol pellets WAXS spectrum and (D) SAXS spectrum, (E) CaSt powder, paracetamol (P) powder, GMS powder, and CaSt–paracetamol–GMS pellets WAXS spectrum and (F) SAXS spectrum, (G) CaSt powder, paracetamol (P) powder, TBC liquid (5%), and CaSt–paracetamol–TBC pellets WAXS spectrum, and (H) SAXS spectrum. (For interpretation of the references to color in this figure legend, the reader is referred to the web version of this article.)

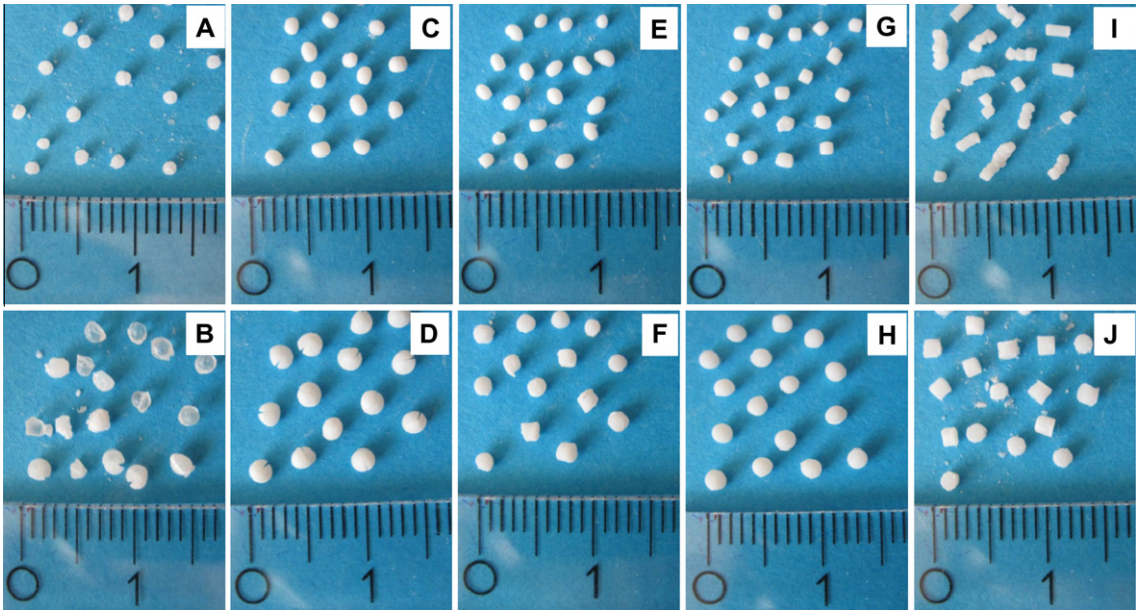

Fig. 4. CaSt pellets produced by HME using a hot-face cutter as downstreaming system: (A) CaSt_1; (B) CaSt_1.5; (C) CaSt/P20%_1; (D) CaSt/P20%_1.5; (E) CaSt/P20%/G5%_1; (F) CaSt/P20%/G5%_1.5; (G) CaSt/P20%/T5%_1; (H) CaSt/P20%/T5%_1.5; (I) CaSt/P20%/T10%_1 and (J) CaSt/P20%/T10%_1.5. (For interpretation of the references to color in this figure legend, the reader is referred to the web version of this article.)

3.4. Effect of plasticizers and drug loading on in vitro dissolution and drug release mechanism

The drug release profiles of the extruded pellets at pH 1.2 and 6.8 are shown in Fig. 5. In Fig. 5A, the melt extruded pellets containing only CaSt and paracetamol (i.e., CaSt/P20%_1, CaSt/P20%_1.5, CaSt/P40%_1, CaSt/P40%_1.5) retarded the drug to a significant extent. With an incorporated drug concentration of 20%, 11.54% paracetamol was released after 8 h. After 24 h, the concentration increased to 47.89%. As expected, the dissolution profile

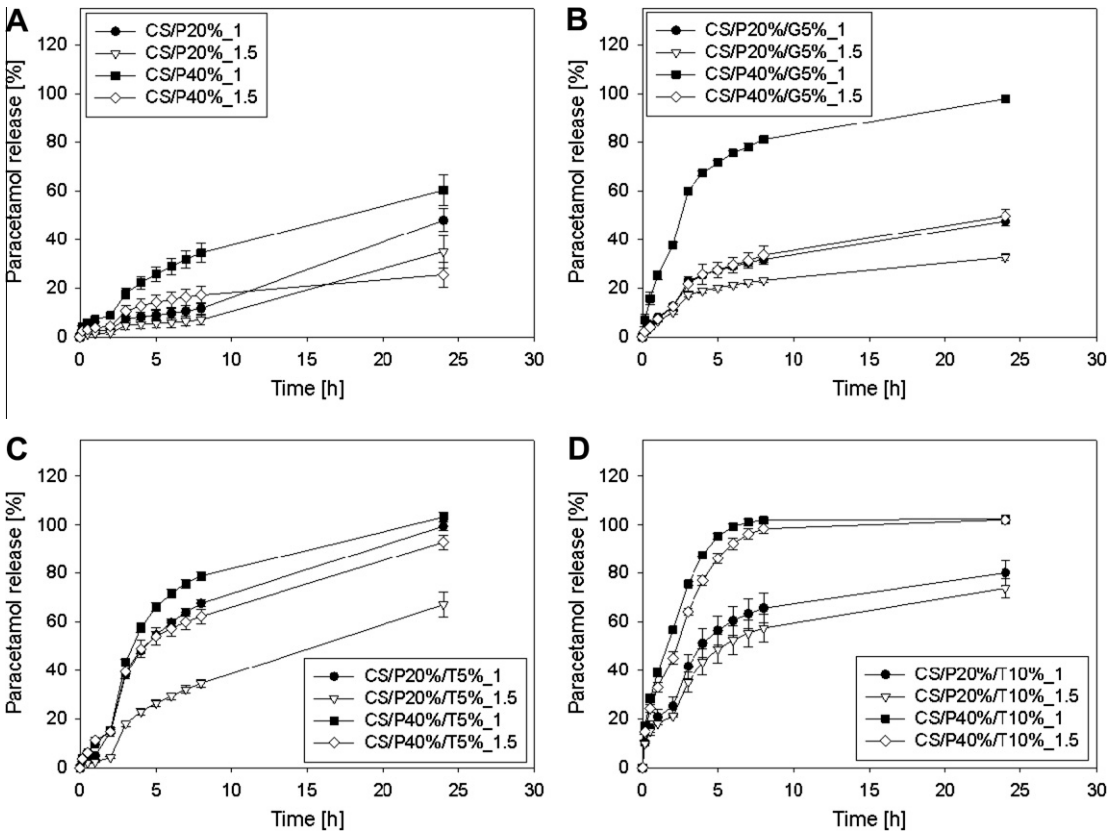

Fig. 5. Release profile depending on particle size, drug content and plasticizing additives. (A) CaSt–paracetamol pellets without plasticizer, (B) CaSt–paracetamol and GMS pellets, (C) CaSt–paracetamol and TBC (5%) pellets, and (D) CaSt–paracetamol and TBC (10%) pellets.

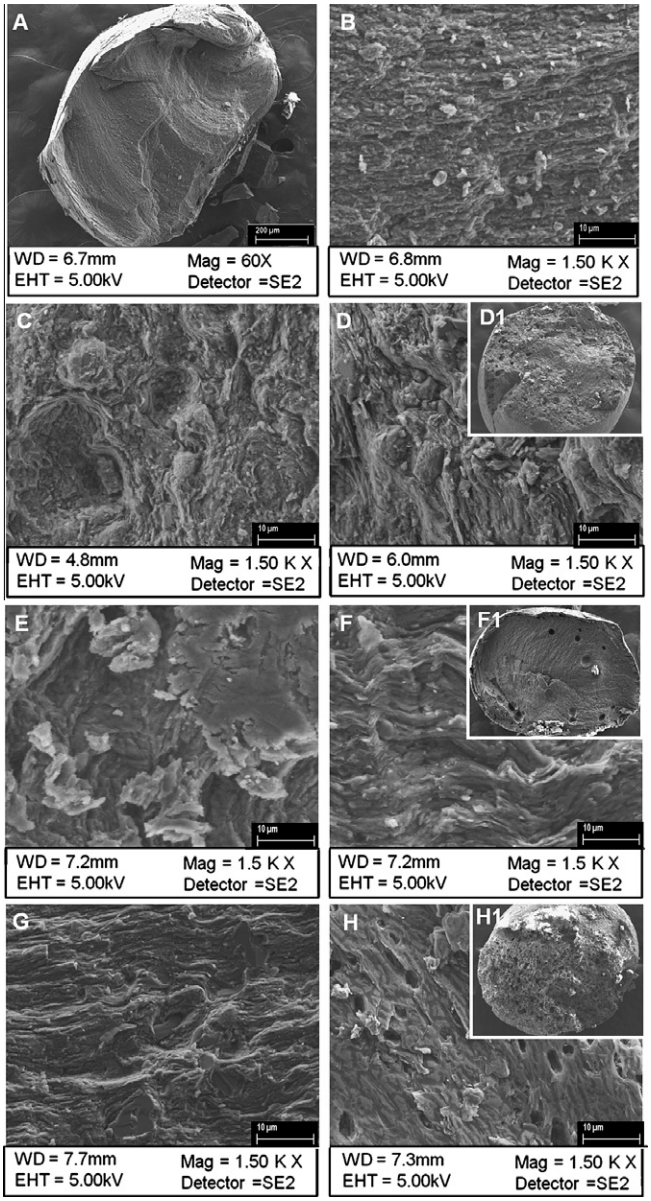

Fig. 6. SEM images of: (A) cross cut of a drug free CaSt pellet and (B) detailed internal structure of a CaSt pellet. Micrographs of drug-loaded pellets before and after 24 h of drug release; (C) detailed internal structure of a CaSt–paracetamol pellet before dissolution; (D) detailed internal structure of the pellet after dissolution, (D1) cross cut of the pellet after dissolution; (E) detailed internal structure of the drug-loaded pellet with GMS and paracetamol before dissolution; (F) detailed internal structure of the pellet after dissolution (F1) cross cut of the pellet after dissolution; (G) detailed internal structure of the drug-loaded pellet with TBC before dissolution; (H) internal structure after dissolution and (H1) cross cut of the pellet after dissolution.

was affected by the pellet size and the drug content. The higher the drug content was, the more paracetamol was dissolved due to an improved water flux through the surface of the melt extruded pellet. After 8 h, 34.36% paracetamol was released and approximately 60% was at the highest value after 24 h. With the increasing size, the release rate decreased. The investigation of the release mechanism revealed that the drug release from paracetamol–CaSt pellets showed release characteristics obeying the diffusion-controlled Higuchi model, r^2 = 0.9930–0.9963.

To enhance drug release from the used matrix system, two plasticizers were investigated since plasticizers may act as controlling agents and influence drug release by modifying the matrix permeability [33]. The dissolution profiles with GMS are illustrated in Fig. 5B. GMS is a low-melting-point material, which is insoluble in water and which is decomposed in the intestinal tract by enzymes. Peh et al. reported that GMS, used for the preparation of wet extruded pellets, retarded the rate of drug release significantly [34]. Later work by Chatchawalsaisin et al. [35] demonstrated that the drug release was controlled by the solubility of the drug and not by GMS, even if the drug was suspended in molten GMS. Our results demonstrate that the addition of GMS increased the drug release to nearly 30% after 8 h and to 47.52% after 24 h (CaSt/P20%/G5%_1). With higher drug amounts (40%, CaSt/P40%/G5%_1), the release rate increased to 80% after 8 h and 97% after 24 h. The investigation of the release mechanism showed that the addition of GMS (CaSt/P20%G5%_1, CaSt/P20%G5%_1.5, CaSt/P40%G5%_1) resulted in a diffusion-controlled release (Higuchi model, r^2 = 0.9937–0.9996). As expected, the release rate was influenced by the pellet size (33% and 49%, respectively).

As a consequence, GMS increased the drug release, probably because GMS exhibits four polymorphs. Among them is an α-form, which is dispersible and which has water-soluble and emulsifying properties, and a β-form, which is suitable for wax matrices to mask bitter taste but has a low wettability. Rapid cooling of melted GMS results in the crystalline α-form [36]. These findings are in agreement with our results. The DSC curves (first heating cycle) displayed an endothermic peak at 63.9 °C with recrystallization after cooling at approximately 50 °C (data not shown). Further studies by Yajima et al. demonstrated that a transformation from the α in β-form is only accelerated at process temperatures of 50 °C [37]. Thus, it can be assumed that (besides the solubility of the API) the influence of GMS on the release behavior of a drug depends on the commercially specified grade of the pure GMS (α or β form) and on the process temperature.

In the next set of experiments, TBC, a liquid plasticizing additive of the citrate ester type, was incorporated into the formulations (see Fig. 5C and D). The concentration of 5% increased the amount of released paracetamol to 65% after 8 h. After 24 h, 100% of the drug was detected in the dissolution medium (CaSt/P20%/T5%_1). The dissolution graphs displayed first-order kinetics (r^2 = 0.9733–0.9913). Due to this increase in drug release, the concentration of TBC was increased to 10%. The dissolution results demonstrated that nearly the same amount of paracetamol was released after 8 h (CaSt/P20%/T10%_1). Differences in the applied TBC concentrations were only observed after 24 h. The release data, however, were best fitted to the Higuchi model, indicating a diffusion-controlled release (r^2 = 0.9771). The most noticeable feature of these results is that with smaller amounts of TBC (5%) the released drug concentration increased to 100%, whereas with 10% TBC no more than 80% of the drug was detected in the dissolution medium. With increasing drug loading, the amount of the released drug increased, and with increasing pellet size, the release rate decreased. These findings indicate that when using CaSt as a matrix carrier combined with higher TBC levels (10%), the released paracetamol concentration does not increase due to the formation of a denser matrix.

In summary, in our study both, GMS and TBC demonstrated the potential to be used as an additive for hot melt extrusion of CaSt. The plasticizing effect on CaSt and impact on drug release from the pellets were higher for TBC. This might be due to (i) a better miscibility and (ii) a high boiling temperature to prevent its loss during processing. Additionally, it appears that the hydrophobic additive is uniformly distributed (emulsified) in the hydrophobic fatty acids (partly interrupting them). Furthermore, it can be concluded that the API liberation of all formulations was mainly governed by a diffusion process.

3.5. Pellet structure

SEM images were taken to study the existence and formation of pores in the examined pellets. The surface and the internal structure of the pellets were evaluated before and after in vitro dissolution (24 h). Pure CaSt showed a smooth, non-porous solidified melt with a great densification of CaSt as shown in Fig. 6A and B. Adding paracetamol resulted in pellets with high density (Fig. 6C). After the dissolution, few pores were found at the surface, indicating that small amounts of the water-soluble drug dissolved in the outer layer. The internal structure of the pellets, however, displayed a non-porous system (Fig. 6D and D1). Incorporating GMS resulted in pellets with high plasticity (Fig. 6E). GMS melted and emulsified in the matrix carrier during extrusion in the α-form. After dissolution, pores were only found close to the surface, which had been generated by the release of the drug and GMS from the CaSt matrix (Fig. 6F and F1). Since GMS is soluble, the number of pores (close to the surface) increased and a higher amount of the drug could be detected in the dissolution medium. The incorporation of TBC, as illustrated in Fig. 6G, also resulted in a smooth, non-porous solidified melt. After dissolving (Fig. 6H), the pellets exhibited clearly more pores in the inner layer (Fig. 6H1) compared to GMS pellets. Due to better miscibility of CaSt with TBC, the dissolution behavior was enhanced and the highest concentration of paracetamol was evaluated, which is in agreement with the results of the in vitro dissolution.

4. Conclusions

Hydrophobic CaSt pellets, including plasticizers and the water-soluble model drug paracetamol, were produced via HME and hot-strand cutting. The findings demonstrate that controlled-release spherical pellets could be successfully prepared via HME, using a hot-strand cutter with two rotating knives as downstreaming system. The thermal behavior of pure CaSt, investigated via DSC, displayed four peaks in the first heating cycle, which were partly reversible on cooling and reproducible at repeated heating. The extrusion process was conducted at temperatures between 100 and 130 °C, since at these temperatures cutable extrudates with a smooth external appearance can be obtained. The effect of two plasticizers on the processibility and the drug release kinetics was investigated. GMS and TBC (less soluble plasticizer) reduced the required process temperature, and extrudates with an appropriate melt viscosity were produced. The tackiness of the strands was slightly increased for TBC resulting in higher ARs. The incorporation of paracetamol into the formulations decreased the ARs due to the decreased formability behavior of the pellets. All paracetamol pellets exhibited ARs $\leqslant 1.28$. As expected, the dissolution profile was affected by the pellet size and the drug content. The release of the API was mainly governed by a diffusion-controlled drug release. Pellets containing no plasticizer exhibited low release rates, attributable to the great densification of the CaSt pellets. The incorporation of GMS increased the drug release. After dissolution, pellets exhibited pores at the surface, which had been generated by the release of the drug and GMS from the CaSt matrix. TBC increased the release rate to the highest extent due to the good miscibility with CaSt. After dissolving, the pellets exhibited pores also in the inner layer. However, increasing TBC levels did not result in an increase in the release rate due to the formation of a denser matrix. SWAXS investigations of the extruded pellets showed that, due to the mechanical treatment of CaSt during extrusion, the order in the crystal lattice increased. No shifting of the peaks occurred in all formulations, demonstrating that CaSt did not melt during the extrusion process and that paracetamol was embedded in the matrix carrier in its crystalline form displaying a solid suspension.

Acknowledgements

The authors thank G.L. Pharma GmbH (Lannach, Austria) for supplying paracetamol and the excipients and Hecus X-Ray Systems, GmbH, Graz, Austria, for providing the S3-MICRO. The authors also thank Dr. P. Pölt, FELMI, Graz, Austria, for his assistance with the electron microscope.

References

[1] K.A. Mehta, G.S. Rekhi, D.M. Parikh, Extrusion/spheronization as a granulation technique, in: D.M. Parikh (Ed.), Handbook of Pharmaceutical Granulation Technology, Taylor & Francis Group, Boca Raton, 2005, pp. 333–363.
[2] H. Kristensen, T. Schaefer, Granulation – a review of pharmaceutical wet-granulation, Drug Dev. Ind. Pharm. 13 (1987) 803–872.
[3] M. Gosau, B.W. Müller, Release of gentamicin sulphate from biodegradable PLGA-implants produced by hot melt extrusion, Pharmazie 65 (2010) 487–492.
[4] M.M. Crowley, B. Schroeder, A. Fredersdorf, S. Obara, M. Talarico, S. Kucera, J. McGinity, Physicochemical properties and mechanism of drug release from ethyl cellulose matrix tablets prepared by direct compression and hot-melt extrusion, Int. J. Pharm. 269 (2004) 509–522.
[5] S. Schilling, N. Shah, A. Malick, J. McGinity, Properties of melt extruded enteric matrix pellets, Eur. J. Pharm. Biopharm. 74 (2010) 352–361.
[6] M.M. Crowley, A. Fredersdorf, B. Schroeder, S. Kucera, S. Prodduturi, M.A. Repka, J. McGinity, The influence of guaifenesin and ketoprofen on the properties of hot-melt extruded polyethylene oxide films, Eur. J. Pharm. Biopharm. 22 (2004) 409–418.
[7] M.M. Crowley, F. Zhang, M.A. Repka, S. Thumma, S.B. Upadhye, S.K. Battu, J.W. McGinity, C. Martin, Pharmaceutical applications of hot-melt extrusion: Part I, Drug Dev. Ind. Pharm. 33 (2007) 909–926.
[8] J. Breitenbach, Melt extrusion: from process to drug delivery technology, Eur. J. Pharm. Biopharm. 54 (2002) 107–117.
[9] M.A. Repka, S.K. Battu, S.B. Upadhye, S. Thumma, M.M. Crowley, F. Zhang, C. Martin, J.W. McGinity, Pharmaceutical applications of hot-melt extrusion: Part II, Drug Dev. Ind. Pharm. 33 (2007) 1043–1057.
[10] E. Doelker, U. Bilati, C.A. Nguyen, S. Galindo-Rodriguez, A.G. Sarraf, Processing of polymeric dosage forms for advanced drug delivery: from melt-extrudates to nanoparticles, Chimia 59 (2005) 336–339.
[11] C.E. Klein, Y.L. Chiu, W. Awni, T. Zhu, R.S. Heuser, T. Doan, J. Breitenbach, J.B. Morris, S.C. Brun, G.J. Hanna, The tablet formulation of lopinavir/ritonavir provides similar bioavailability to the soft-gelatin capsule formulation with less pharmacokinetic variability and diminished food effect, JAIDS – J. Acq. Immune Def. Synd. 44 (2007) 401–410.
[12] D.A. Miller, J.T. McConville, W. Yang, R.O. Williams, J.W. McGinity, Hot-melt extrusion for enhanced delivery of drug particles, J. Pharm. Sci. 96 (2007) 361–376.
[13] J. Krause, M. Thommes, J. Breitkreutz, Immediate release pellets with lipid binders obtained by solvent free extrusion, Eur. J. Pharm. Biopharm. 71 (2009) 138–144.
[14] W.L. Chiou, S. Riegelman, Pharmaceutical applications of solid dispersion systems, J. Pharm. Sci. 60 (1971) 1281–1302.
[15] L.J. Thomsen, T. Schaefer, H.G. Kristensen, Prolonged release matrix pellets prepared by melt pelletization II. Hydrophobic substances as meltable binders, Drug Dev. Ind. Pharm. 20 (1994) 1179–1197.
[16] H.G. Schroeder, A. Dakkuri, P.P. DeLuca, Sustained release from inert wax matrixes I: drug–wax combinations, J. Pharm. Sci. 67 (1978) 350–353.
[17] H. Sato, Y. Miyagawa, T. Okabe, M. Miyajima, H. Sunada, Dissolution mechanism of diclofenac sodium from wax matrix granules, J. Pharm. Sci. 86 (1997) 929–934.
[18] Y. Miyagawaa, T. Okabea, Y. Yamaguchia, M. Miyajimaa, H. Sato, H. Sunada, Controlled-release of diclofenac sodium from wax matrix granule, Int. J. Pharm. 138 (1996) 215–224.
[19] R.C. Row, P.J. Shesky, M.E. Quinn, Handbook of Pharmaceutical Excipients, sixth ed., Pharmaceutical Press, 2009.
[20] E. Roblegg, S. Ulbing, S. Zeismann, A. Zimmer, Development of lipophilic calcium stearate pellets using ibuprofen as model drug, Eur. J. Pharm. Biopharm. 75 (2010) 56–62.
[21] R. Arshady, Microspheres and microcapsules, a survey of manufacturing techniques: Part III. Solvent evaporation, Polym. Eng. Sci. 30 (1990) 915–924.
[22] O. Glatter, Small Angle X-ray Scattering, Academic Press, London, 1982.
[23] P. Costa, J.M. Sousa Lobo, Modeling and comparison of dissolution profiles, Eur. J. Pharm. Sci. 13 (2001) 123–133.
[24] G.S. Hattiangdi, M.J. Vold, R.D. Vold, Differential thermal analysis of metal soaps, Ind. Eng. Chem. 41 (1948) 2320.
[25] R.D. Vold, J.D. Grandine, M.J. Vold, Polymorphic transformations of calcium stearate and calcium stearate monohydrate, J. Colloid Sci. 3 (1948) 339.

[26] P. Garnier, P. Gregoire, P. Montmitonnet, F. Delamare, Polymorphism of crystalline phases of calcium stearate, J. Mater. Sci. 23 (1988) 3225–3231.
[27] V. Dubinsksaya, N. Polyakov, Y. Suponitskii, N. Dement'eva, V. Bykov, Studies of moisture exchange between stearic acid, calcium stearate, and magnesium stearate, Pharm. Chem. J. 44 (2010) 89–93.
[28] S. Qi, A. Gryzke, P. Belton, D.Q.M. Craig, Characterisation of solid dispersions of paracetamol and EUDRAGIT® E prepared by hot-melt extrusion using thermal, microthermal and spectroscopic analysis, Int. J. Pharm. 34 (2008) 158–167.
[29] C. de Brabander, G. van den Mooter, C. Vervaet, J.P. Remon, Characterization of ibuprofen as a nontraditional plasticizer of ethyl cellulose, J. Pharm. Sci. 91 (2002) 1678–1685.
[30] T. Mezger, Das Rheologie Handbuch: für Anwender von Rotations- und Oszillations-Rheometern, Vincentz Verlag, Hannover, 2000.
[31] C. Reitz, P. Kleinebudde, Spheronization of solid lipid extrudates, Powder Technol. 189 (2009) 238–244.
[32] R. Chopra, F. Podczeck, J.M. Newton, G. Alderborn, The influence of pellet shape and film coating on the filling of pellets into hard shell capsules, Eur. J. Pharm. Biopharm. 53 (2002) 327–333.
[33] N.A. Ghebremeskel, C. Vernavarapu, M. Lodaya, Use of surfactants as plasticizers in preparing solid dispersions of poorly soluble API: stability testing of selected solid dispersions, Pharm. Res. 23 (2006) 1928–1936.
[34] K.K. Peh, K.H. Yuen, Development and in-vitro evaluation of a novel multiparticulate matrix controlled release formulation of theophylline, Drug Dev. Ind. Pharm. 21 (1995) 1545–1555.
[35] J. Chatchawalsaisin, F. Podzeck, J.M. Newton, The preparation by extrusion/spheronization and the properties of pellets containing drugs, microcristalline cellulose and glycerolmonostearate, Eur. J. Pharm. Biopharm. 24 (2005) 35–48.
[36] T. Yajima, S. Itai, H. Takeuchi, Y. Kawashima, Determination of optimum processing temperature for transformation of glyceryl monostearate, Chem. Pharm. Bull. 50 (2002) 1430–1433. Tokyo.
[37] T. Yajima, S. Itai, H. Takeuchi, Y. Kawashima, Optimum heat treatment conditions for masking the bitterness of the clarithromycin wax matrix, Chem. Pharm. Bull. 51 (2003) 1223–1226. Tokyo.